Dynamic Geo-Fencing for Polycentric Congestion Management

A Simulation-Based Analysis

Pecorari, Nirvana; Rinaldi, Marco; Hoogendoorn, Serge

DOI
10.1109/MT-ITS56129.2023.10241647

Publication date
2023

Document Version
Final published version

Published in
2023 8th International Conference on Models and Technologies for Intelligent Transportation Systems, MT-ITS 2023

2023 8th International Conference on Models and Technologies for Intelligent Transportation Systems (MT-ITS) | 978-1-6654-5530-5/23/$31.00 ©2023 IEEE | DOI: 10.1109/MT-ITS56129.2023.10241647

Dynamic Geo-Fencing for Polycentric Congestion Management: A Simulation-Based Analysis

1st Nirvana Pecorari
Department of Transport and Planning
Delft University of Technology
Delft, The Netherlands
N.Pecorari@tudelft.nl

2nd Marco Rinaldi
Department of Transport and Planning
Delft University of Technology
Delft, The Netherlands
0000-0001-7027-7548

3rd Serge Hoogendoorn
Department of Transport and Planning
Delft University of Technology
Delft, The Netherlands
0000-0002-1579-1939

***Abstract*—Our cities are growing at an unprecedented pace. The flexible use of metropolitan infrastructures is the key to maintaining, if not increasing, the current quality of life. The combined use of geo-fence technology and connected vehicles can be the tool to achieve this flexibility. In this paper, we take a first step in the evaluation of the benefits that dynamic geo-fencing could bring. In a simulation-based environment, we employ a computer vision approach to dynamically identify congested areas in a given transportation network. We then compare the performance of perimeter control based on dynamic geo-fencing vs conventional perimeter strategies, based on a fixed, pre-determined area – a scenario mimicking traffic management approaches currently deployed in large metropolitan areas worldwide. Simulation results highlight a reduction of more than 20% of the Total Time Spent in a regular Manhattan grid network, encouraging further efforts to validate the efficiency of dynamic geo-fencing in addressing externalities (congestion, pollution, noise, etc.) in more realistic scenarios.**

***Index Terms*—congestion management, geo-fencing, perimeter control, Macroscopic Fundamental Diagram (MFD)**

I. Introduction & Literature Review

Our cities are growing at an unprecedented pace, largely unmet by infrastructure expansion due to constraints related to budgetary restrictions, spatial constraints, and last but not least, the risk of induced demand, nullifying supply expansion efforts. Faced with these issues, redesigning the *way* we conceive the current urban environment becomes crucial. The management of road infrastructure plays a fundamental role in bridging the gap between growing demand and limited supply. Among these management strategies, perimeter control has been identified as a promising solution to address issues such as congestion during peak hours, and has therefore received considerable interest by researchers and practitioners in the last decades. As will be detailed later, one of the key assumptions underlying currently deployed approaches – as well as the vast majority of research efforts – is that the location and size of said perimeters are exogenous design parameters, chosen a-priori by the involved stakeholders. The fundamental hypothesis underlying this work is that static design inherently hampers perimeter control strategies' potential in addressing externalities in different locations at different times (i.e. flexible). Shifting to time-varying location-based handling of transportation supply infrastructure, we believe, is the key to maintaining, if not increasing, the current quality of life in metropolitan areas. For example, school zones might benefit from dynamic access policies, so that capacity and accessibility are restricted only at specific times of the day; similarly, reactive identification of an area affected by a road accident, and reduction of inflow in it, might improve safety during rescue operations [14].

The widespread adoption of information and communication technologies and the resulting increasing penetration rate of Connected Vehicles (CV), is a building block upon which such flexibility can be based. In the specific instance of perimeter control, we believe geo-fencing to be most promising. Thanks to this technology, virtual perimeters that enclose real-world geographical areas of interest can be drawn, digitally, based on GPS coordinate systems. In combination with GPS location data collected and communicated by connected vehicles, these digital borders can be employed to assess whether or not a given vehicle is entering a protected area. This information could then be employed, in combination with appropriately developed traffic management techniques, to dynamically regulate the inflow (outflow) of vehicles in any arbitrary subdivision of the transportation network, without requiring location-bound physical infrastructure (e.g. gantries).

Perimeter management techniques must be overhauled to take full advantage of such added flexibility. In particular, we identify three key necessary extensions: 1) *dynamic* identification of areas requiring intervention, 2) dynamic intervention strategies, and 3) *dynamic* communication with road users. We review these three elements in the following points.

1) defining key performance indicators (KPIs) is of paramount importance in identifying areas for intervention. We believe that traffic congestion (together with traffic externalities like pollution and noise, object of future research) represents an important livability index for a metropolitan area. Moreover, the time-varying KPIs values must be kept in the set of values that are considered acceptable by e.g the policy makers. On the basis of these KPIs, it is interesting to identify regions of the network where values exceed the set of acceptable values. We dub these regions *critical*.

978-1-6654-5530-5/23/$31.00 ©2023 IEEE

2) identifying critical regions, and applying a traffic management strategy to maintain associated KPIs with the corresponding set of acceptable values are key challenges for urban management. To date, perimeter control is a strategy to address problems of congestion, pollutant emissions, and safety within fixed areas by monitoring the entry flow at the perimeters, and holding vehicles outside the controlled areas, if necessary [6] [7] [8] [9]. Moreover, the introduction of the Macroscopic Fundamental Diagram (MFD) enabled a promising direction toward the management of systematic congestion at the network level at a very low computational cost perimeter flow control [2].
3) dynamic and seamless communication can be ensured by navigation advice broadcast through in-car systems. Dynamic avoidance maps, introduced and described in [13], may represent an important first step in this direction.

The application of perimeter control to dynamically defined perimeters differs from the traffic management strategies currently implemented in large metropolitan areas worldwide, such as London, Stockholm, and Milan. In fact, since the first decade of this century, these areas have adopted a management strategy consisting of applying perimeter control to Central Business Districts, to address congestion and pollution therein [5]. The exogenous choice of location and size of said perimeters prevents the network control paradigm from rapidly responding to the KPIs' temporal evolution.

Dynamic identification of areas of interest, point 1), finds its counterpart in the literature under the name of "dynamic network partitioning". Recent studies have successfully implemented and tested combined dynamic partitioning and perimeter control approaches to mitigate congestion. In particular, [1] introduces a perimeter control method wherein the region boundaries adapt in real-time to tackle the propagation of local congestion pockets. By construction, its approach is not designed to cope with polycentric congestion situations efficiently. Conversely, [2] adopts a graph-convolution-based method for network partitioning, where it uses a clustering method capable of determining network partitions in terms of a prefixed number of clusters, three in its case: high, medium, and low density, corresponding to the three regions of the NMFD. This approach prevents maximal flexibility in identifying critical areas of the network; in fact, in order to address more externalities (congestion, pollution, noise, etc.), it is important for us to be able to vary the set of acceptable values over time (hours or days).

Consequently, in Sec. III, we design a time-varying location-based computer vision-based approach to partition a metropolitan area into approximately homogeneous regions in terms of traffic congestion, using vehicle density and the total time these spend in the network (TTS) as indicators. To the best of our knowledge, this is the first study involving a dynamic partitioning methodology that

1) is not constrained to spatial connectivity requirements of the partitions, nor to a pre-partition of the network;
2) does not require increased computational time, for instance due to re-training, when changing the value of free parameters;
3) is not developed starting from a pre-identified hotspot region, as in [15].

These are crucial features for a seamless solution to the problem described above, formalized in Sec. II.

Maintaining the artificial network and demand profile, we simulate three scenarios: uncontrolled, fixed-controlled, and dynamically controlled. In the first, in Sect. IV-B, no control strategy is adopted. Then, in Sec. IV-C, we set a scenario that resembles the current traffic management strategy described above: MFD-based control strategy modifies the inflow of a fixed-congested area of the network. Lastly, in Sec. IV-D we design a scenario where we apply the MFD-based control strategy to congested regions of the networks, dynamically identified through the heatmaps of the congestion. Total Time Spent (TTS) is an indicator capable of measuring network congestion. We use the TTS to assess whether the proposed dynamic partitioning methodology, together with the MFD-based control strategy, is more beneficial than the currently used fixed partitioning of the network. We finally draw concluding remarks and recommendations for future research in Sec. V.

II. Problem formulation

We identify a transport network G with a directed graph. We define V as the set of nodes of G, and $\mathcal{L}$ the set of links of G, where $l = [(x_s^l, y_s^l), (x_t^l, y_t^l)]$ is a element $\in \mathcal{L}$, with $(x_s, y_s) \in V$ a source node and $(x_t, y_t) \in V$ a target node. We call R the set of all the possible topologically connected subdivisions of G, comprising at least 3 nodes and 3 links. We define $\rho(\mathbb{R}^3, \mathbb{R})$ a function associating a level of congestion ρ [veh/km] to each triplet of spatio-temporal coordinates (x, y, k), and a corresponding time-invariant set of acceptable values (see Sec. I), $[0, \rho_{max}]$. We label as critical nodes V_c nodes for which $\rho(x, y, k) > \rho_{max}$ holds, at time k. The set of critical nodes, and the links having as the source and target node critical nodes, compose the critical region $R_c \subset R$. Finally, a metering controller is applied at the source node of the links that are connected with a link having only the target node in the critical region. We call L_e the set of the equipped links of R_c.

We assume the regions in R to be homogeneous in terms of congestion distribution. As such, a well-defined MFD that relates each region's production p to regional accumulation $n(k)$ is assumed to be a sufficiently accurate model allowing to macroscopically capture the dynamics of the traffic of each region. Adapting [3], we define the accumulation of a region R_c at time k, $n(k)$, the weighted average density calculated as follows:

$$n(k) = \frac{\sum_{l \in R_c} (\rho^l(k) \ell^l)}{\sum_{l \in R_c} \ell^l}, \tag{1}$$

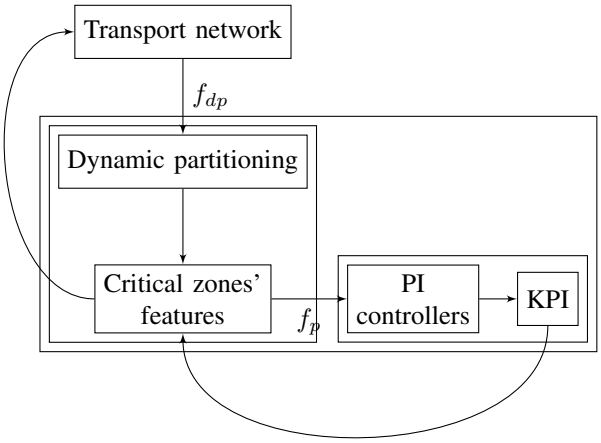

Fig. 1. Combined scheme of dynamic network partitioning and control strategy actuated by PI controllers.

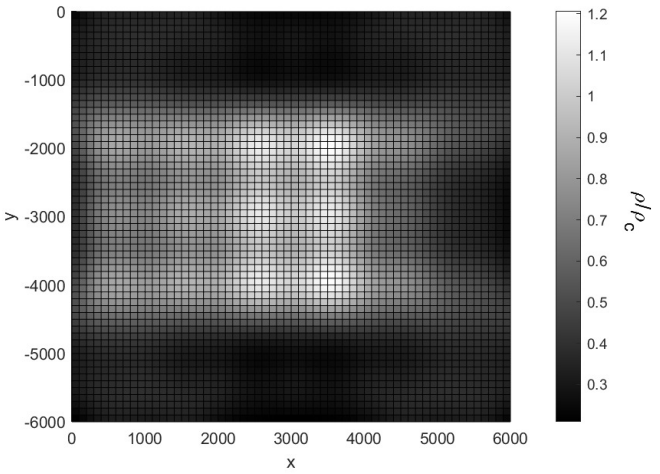

Fig. 2. Example of density heatmap of the network.

where q^l, ρ^l and ℓ^l are the flow, density and length of link l, respectively. Furthermore, we define the critical accumulation of the region R_c, n^*, as follows:

$$n^* = \frac{\sum_{l \in R_c} \left(\frac{cap^l}{v_f^l} \ell^l \right)}{\sum_{l \in R_c} \ell^l}, \tag{2}$$

where cap^l and v_f^l are the capacity and the free flow speed of link l, respectively. Finally, adapting [3], we define production in a region R_c at time k, $p(k)$, as the weighted average flow:

$$p(k) = \frac{\sum_{l \in R_c} (q^l(k) \ell^l)}{\sum_{l \in R_c} \ell^l} \tag{3}$$

Given T_s the time interval, N_U^l and N_D^l the cumulative number of vehicles counted on link l upstream and downstream ends, respectively, we formalize our management strategy as follows: *at each time step k, on which sub-set of regions is it best to apply perimeter control so that Total Time Spent (5) is minimized?*

$$\underset{\{R^1, R^2, \ldots, R^{i_{max}}\} \subset R}{\operatorname{argmin}} \sum_{i=1}^{n} TTS_{R^i}(u(k)) \tag{4}$$

$$TTS_{R^i}(u(k)) = \sum_{l \in L^i} \left(\int_0^k N_U^l(\tau, u(k)) d\tau - \int_0^k N_D^l(\tau, u(k)) d\tau \right) \cdot T_s \tag{5}$$

Where $u(\cdot)$ is the MFD-based perimeter control action, as defined in (8).

III. Methodology

In this section, we provide an overview of the combined use of dynamic partitioning (Sec. III-A) and perimeter control MFD-based (Sec. III-B) we propose as a feasible and seamless solution to the problem we introduced in Sec. I, and formalized in Sec. II. The combined approach is depicted in Fig. 1. We will evaluate the performance of this approach in Sec. IV.

A. Dynamic network partitioning

The dynamic partitioning of the network is performed following three steps: 1) we associate the transport network graph G with a heatmap of the selected KPI (congestion, ρ); 2) we identify areas of interest for the application of our time-dependent perimeter control; 3) we apply an area size-based filter. We explain these three steps in further detail in the following.

1) Heat map: We model the geographical distribution of our chosen KPI(s) as a mixture of Gaussian distributions, adopting an approach similar to that underlying Gaussian Mixture Models (GMMs).

In order to obtain the mixture of Gaussian distributions, we first associate the transport network's graph G with a mesh grid with extremes $[X_{min}, X_{max}]$, $[Y_{min}, Y_{max}]$ and A_M as the mesh size. Then, with a frequency f_{dp} (in min^{-1}), we associate a 3-dimensional symmetric Gaussian with each link $l \in \mathcal{L}$. As described in 6, each Gaussian function's centroid is located at the link's midpoint $\bar{P}_l = (\bar{x}_l, \bar{y}_l)$, and the maximal Z-value, after normalization, is equal to the ratio between the density of vehicles on the link l, ρ_l, at time k, and the critical density of the link l, ρ_c^l.

$$G^l(k) = \frac{\rho^l(k)/\rho_c^l}{\sigma\sqrt{2\pi}} \exp - \frac{(x - \bar{x}_l)^2 + (y - \bar{y}_l)^2}{2\sigma^2} \tag{6}$$

This ensemble yields a heat map of the chosen KPI at the time k. This approach is multipurpose given that, in principle, we can quickly develop heat maps of different KPIs, and combine them (see Sec. V). We show an example in Fig. 2.

2) Z-cut: To determine critical zones R_c we must choose a criticality threshold $\tilde{z} = \tilde{\rho}^l/\rho_c^l$, which corresponds to a plane described by

$$z = \tilde{z}. \tag{7}$$

Thanks to the continuity properties of Gaussian mixtures, the intersection between the plane (7) and the density heatmap

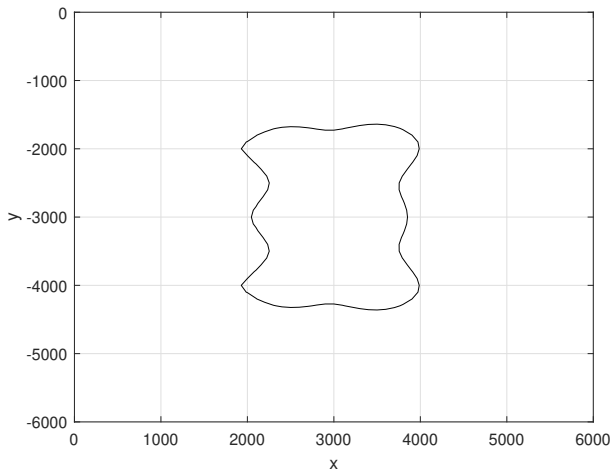

Fig. 3. Example of zone contouring from the heatmap. With $\tilde{z} = 0.9$ as threshold, and deleting regions with area $< \tilde{A}$, with $\tilde{A} = 10^6$.

surface will result in zero, or more, closed, continuous curves in the xy plane, representing the (dynamic) area(s) to be subjected to perimeter control, as exemplified in Fig. 3.

As will be detailed later, in our experiments we choose a value of $\tilde{z}$ such that the initial critical region is comparable among the tested scenarios. In practical instances, $\tilde{z}$ should be chosen considering the specific needs of the metropolitan area, in relation to policy objectives. We note that, due to the way the heatmap is constructed, there is only a *approximate* correspondence between the ρ/ρ_c value associated with a point of the mesh grid and the exact ρ/ρ_c value measured on the underlying network.

3) Filtering: Finally, we filter the detected candidate areas for perimeter control according to their geometric area [m^2]: we set a threshold value for the area of a region, R_c^i, and maintain only the regions that have area $A \geq \tilde{A}$. This ensures that candidate critical regions for perimeter control adhere to our definition of regions as detailed in Sec. II (minimum quantity of affected nodes and links). Therefore, in our experiments we choose a threshold value $\tilde{A} = 10^6$, which corresponds to the area of a square in the mesh grid.

B. Controller design

The inflow of vehicles entering R_c^i at time k is modulated, with a frequency f_p (in min^{-1}), using a perimeter control, through a set P^i of PI controllers. We define P_m^i as a generic PI controller for the critical zone R_c^i, at time k. Each P_m^i is located at the downstream end of the equipped links $l \in L_e$.

Following previous work in MFD-based feedback perimeter control [4], we compute the control signal $u(k)$ of each PI controller as follows:

$$u(k) = -KP\left(n^i(k) - n^i(k-1)\right) + KI\int_0^t \left(n^i(k) - n_{sp}\right) dk \tag{8}$$

with KI, $KP \in \mathbb{R}^+$ respectively the integral and proportional feedback gain factors. We assess the impact of these two parameters through sensitivity analysis in Sec. IV-E.

The control signal determines the percentage of outgoing flow on the link $l \in L_c^i$ that is allowed to cross into the critical region R_c. The general control action of the PI controller at time k on link l, $c^l(k)$ is as follows:

$$c^l(k) = \frac{q(k-1) + u(k)}{cap^l}, \tag{9}$$

and consequently the admissible flow $q^l(k)$ is computed as:

$$q^l(k) = \min(q^l(k-1), c^l(k)q^l(k-1)). \tag{10}$$

IV. Experiments

In this section, we apply the proposed perimeter control based on dynamic zoning, described in III. We assess its effectiveness by comparison to two other scenarios: uncontrolled, in IV-B, and with a perimeter control based on a static zoning, in IV-C. We validate our approach through a simulation-based framework, implemented in Mathworks®MATLAB™. Specifically, we employ the Iterative Link Transmission Model approach of [11], accompanied by a Dynamic User Optimum route choice framework, which, at each simulation step, allocates users to paths following a multinomial logit approach, based on instantaneous travel times.

A. Experimental setup

We consider a scenario featuring a fully bidirectional Manhattan-like network grid, consisting of 7x7 regularly spaced squares. Origins and destinations are located at the entry and exit links at the network's borders. In total, we consider 28 origins (O) and 28 destinations (D) centroids. All links l have a length ℓ^l of 1 km $\pm\, \epsilon$, where $\epsilon \sim U(-0.001, 0.001)$ is a numerical perturbation introduced to avoid excessive symmetry during the equilibrium assignment phase to all links l except those serving the central horizontal OD couples (15↔21, 22↔28, 29↔35). The links that serve the central horizontal OD couples have a free flow speed v_f^l of 50 km/h, while the speed is limited to 30 km/h for the rest of the network. All links have a capacity cap^l of 600 veh/h, except the six thicker links, which have a capacity of 400 veh/h. All links have a jam density k_j of 45 veh/km/lane, except for the six thicker links, which have a k_j of 30 veh/km/lane.

These design choices trigger a specific property: for suitable demand values, the bottlenecks highlighted in Fig. 4 will activate, causing severe spillback and congestion, possibly influencing adjacent OD couples. We simulate a total of 4 h of operations, considering a time discretization interval $T_s = 1$ min, with constant demand entering the network at time $k = 0$, and lasting up to $k = 120$, i.e. for a total simulated duration of 2 hours. During this period, the demand is 225 veh/h for each OD couple, except for couples (15↔21, 22↔28, 29↔35), for which the demand is 600 veh/h. For the remainder of the simulation time, no demand enters the network.

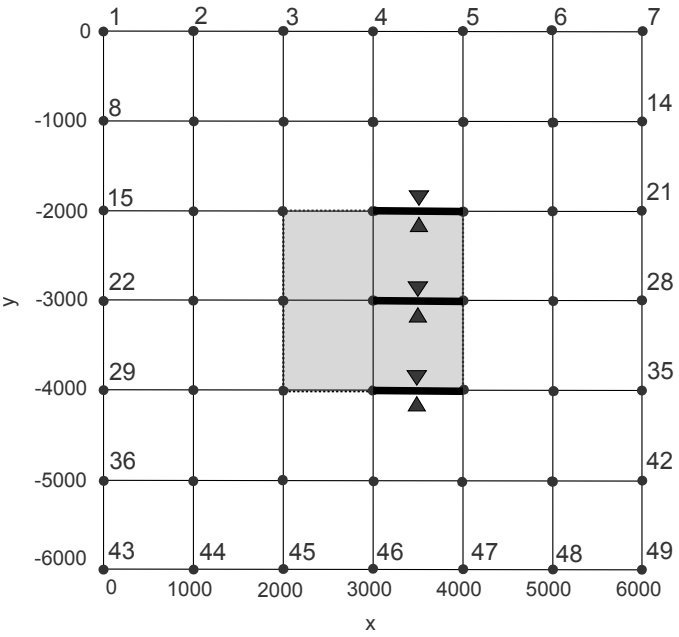

Fig. 4. Case study road network.

B. Uncontrolled case

In this scenario, no control action is taken, and vehicles are therefore free to distribute throughout the network according to equilibrium principles. We show the resulting MFD in Fig. 5. The network exhibits considerable congestion without any management intervention, with no discernible recovery patterns in the MFD diagram. This is further reinforced by the comparative Total Time Spent results of Fig. 7 (dotted gray line).

C. Fixed controlled case

In this scenario, at $k = 0$ we define the critical regions i_{max} R_c^i, to be controlled through perimeter control, as described in Sec. III-B. The number i_{max} is constant over time. We also define the location, size, and shape of the critical area(s) R_c^i. We show the critical region R_c^1 ($i_{max} = 1$) in Fig. 4, in gray. We define for the PI controller a set point of $n_{sp} = 1.8n^{*i}$, and $KP = KI = 10$. We will perform a sensitivity analysis on the two gains in Sec. IV-E. We show in Fig. 6 the MFD of the critical region R_c^1 in the uncontrolled case, and in the case where the controller modulates the inflow of the critical region during the entire simulation time. The critical pre-fixed area shows considerable congestion without any management intervention (ground case); this justifies the use of (MFD-based) perimeter control. The fixed-area controller can successfully reduce the severity of congestion in the protected area, as highlighted by the lower occurrence of high accumulation measurements in the region's MFD. The network's Total Time Spent is also reduced, as shown in Fig. 7 (solid gray line).

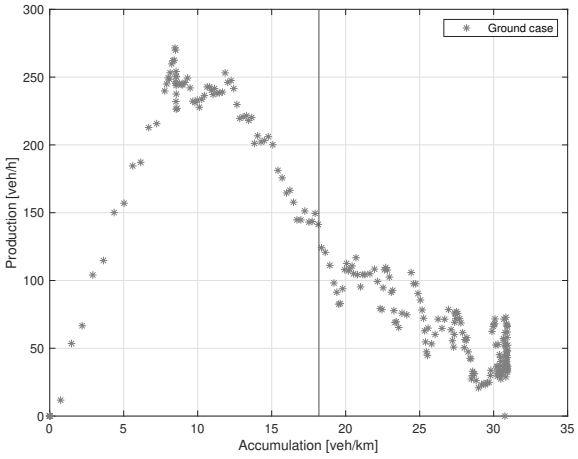

Fig. 5. MFD of the network in the uncontrolled scenario. The solid vertical line indicates the future controller set point accumulation, $n_{sp} = 18$ veh/km.

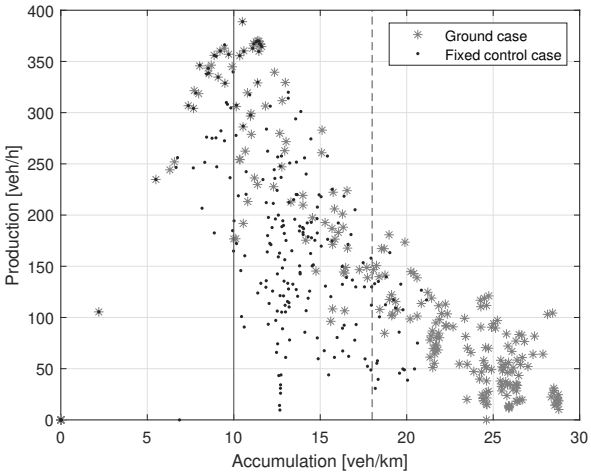

Fig. 6. MFD of zone R_c^1 in the Fixed controlled case. Critical accumulation n^{*1} and controller set point n_{sp} are shown respectively as solid and dashed lines.

D. Dynamic controlled case

In this scenario, we test our proposed dynamic partitioning scheme. Starting from $k = 0$, with a frequency $f_{dp} = 4/60$ min^{-1}, regions with an overall $\rho/\rho_c \geq \tilde{z}$ become critical. We assume $\tilde{z} = 0.9$ Each critical region R_c^i is controlled by an independent, memory-less PI controller P_n, with $KI = KP = 10$ and $n_{sp} = 1.8n^{*i} \forall P_n$, with $f_p = 1/60$ min^{-1}.

In these experiments, while little difference is found between the three scenarios during the onset and build-up of congestion, recovery seems to be substantially affected by the different control scenarios. Specifically, maintaining fixed-area control during the recovery phase seems to be counter-productive – our proposed dynamic approach is capable of recognizing this effect and thereby leads to faster recovery times and overall reduced Total Time Spent.

Moreover, the Manhattan grid network we used for the simulations is relatively small in size, allowing congestion to spread over an area that actually represents *large* part

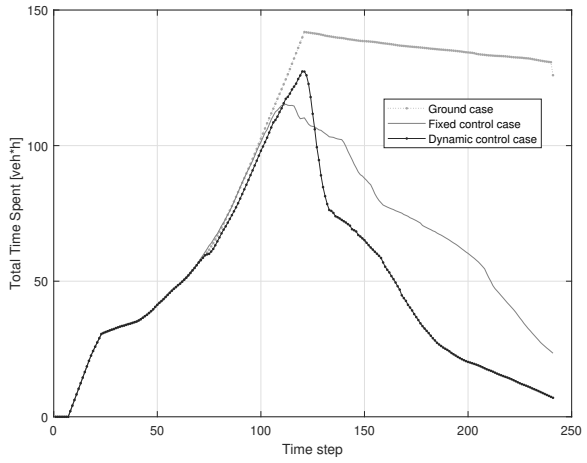

Fig. 7. Total Time Spent evolution for the three test scenarios.

of the network. Due to this, in the time range 110-125, in the dynamic-controlled case, control actions do not exist (the controlled area does not allow the existence of links l to be controlled (see Sec. II), whereas the presence of controlled links is always guaranteed by the fixed-controlled approach.

E. Sensitivity analysis

In this section, we evaluate the performance of PI controllers under different values of KP, KI, for the no control (A), fixed control (B), and dynamic control (C) scenarios. We show the results in Tab. I.

TABLE I
TTS IMPROVEMENT (%) B VS A AND C VS A, VARYING KI AND KP VALUES

KP KI	TTS improvement B vs A	TTS improvement C vs A
50 0	16%	42%
0 50	36%	50%
50 50	36%	50%
100 0	32%	38%
0 100	36%	50%
100 100	36%	50%

V. SUMMARY AND FUTURE RESEARCH

In this paper, we took a first step in assessing the potential benefits that dynamic perimeter control based on geo-fencing techniques can bring to transportation networks. A dynamic network partitioning approach was implemented, based on an elementary computer vision approach, through which we could simulate a flexible and responsive network management approach. The evolution of the network's TTS in the third scenario (Fig. 7) shows the effectiveness of the accumulation-based perimeter control strategy applied to a time-varying set of subregions in addressing polycentric congestion, improving the network's TTS by more than 20% compared to a fixed-region approach.

The results of this study encourage further efforts to validate the efficiency of dynamic geo-fencing in addressing traffic externalities (congestion, pollution, noise, etc.), considering real-life networks and field data, as well as tailoring control parameters for each critical region, to fully exploit the degrees of freedom proper of dynamic geo-fencing. Finally, a strong assumption underlying this work is that, as long as a given network exhibits a well-defined MFD, this property will hold for arbitrary non-trivial partitions of the network itself. Determining the necessary and sufficient conditions for which this assumption is shown to hold represents a key future research direction.

REFERENCES

[1] Jiang, S., Keyvan-Ekbatani, M., Ngoduy, D. (2022). Partitioning of urban networks with polycentric congestion pattern for traffic management policies: Identifying protected networks. Computer-Aided Civil and Infrastructure Engineering.

[2] Li, Y., Mohajerpoor, R., Ramezani, M. (2021). Perimeter control with real-time location-varying cordon. Transportation Research Part B: Methodological, 150, 101-120.

[3] Knoop, V. L., Van Lint, H., Hoogendoorn, S. P. (2015). Traffic dynamics: Its impact on the macroscopic fundamental diagram. Physica A: Statistical Mechanics and its Applications, 438, 236-250.

[4] Åström, K. J. (2002). Control system design lecture notes for me 155a. Department of Mechanical and Environmental Engineering University of California Santa Barbara, 333.

[5] Croci, E. (2016). Urban road pricing: a comparative study on the experiences of London, Stockholm and Milan. Transportation Research Procedia, 14, 253-262.

[6] Ding, H., Zhou, J., Zheng, X., Zhu, L., Bai, H., Zhang, W. (2020). Perimeter control for congested areas of a large-scale traffic network: A method against state degradation risk. Transportation Research Part C: Emerging Technologies, 112, 28-45.

[7] Guo, Q., Ban, X. J. (2020). Macroscopic fundamental diagram based perimeter control considering dynamic user equilibrium. Transportation Research Part B: Methodological, 136, 87-109.

[8] Ren, Y., Hou, Z., Sirmatel, I. I., Geroliminis, N. (2020). Data driven model free adaptive iterative learning perimeter control for large-scale urban road networks. Transportation Research Part C: Emerging Technologies, 115, 102618.

[9] Su, Z. C., Chow, A. H., Zheng, N., Huang, Y. P., Liang, E. M., Zhong, R. X. (2020). Neuro-dynamic programming for optimal control of macroscopic fundamental diagram systems. Transportation Research Part C: Emerging Technologies, 116, 102628.

[10] Jiang, S., Keyvan-Ekbatani, M., Ngoduy, D. (2021). A model predictive perimeter control with real-time partitions. IFAC-PapersOnLine, 54(2), 292-297.

[11] Himpe, W., Corthout, R., Tampère, M. C. (2016). An efficient iterative link transmission model. Transportation Research Part B: Methodological, 92, 170-190.

[12] Tampère, C. M., Corthout, R., Cattrysse, D., Immers, L. H. (2011). A generic class of first order node models for dynamic macroscopic simulation of traffic flows. Transportation Research Part B: Methodological, 45(1), 289-309.

[13] Leclercq, L., Ladino, A., Becarie, C. (2021). Enforcing optimal routing through dynamic avoidance maps. Transportation Research Part B: Methodological, 149, 118-137.

[14] European Institute of Innovation and Technology (EIT). EIT Urban Mobility, 2021. https://www.eiturbanmobility.eu/projects/code-the-streets-future-digital-mobility-management/. Last accessed on November 14, 2022.

[15] Hamedmoghadam, H., Zheng, N., Li, D., Vu, H. L. (2022). Percolation-based dynamic perimeter control for mitigating congestion propagation in urban road networks. Transportation research part C: emerging technologies, 145, 103922.